Neutron Spectrometer and Neutron Counting Diagnostics for General Fusion's LM26 Machine

generalfusion

A.J. Radich[1], R. Underwood[1,2], F. Retière[2], K. Starosta[3], M.T. Hildebrand[1],
P. Carle[1], L. Packer[4], S. Bradnam[4], T. Eade[4], H. Chohan[4]

[1]General Fusion Inc., Richmond, BC, Canada, [2]TRIUMF, Vancouver, BC, Canada,
[3]Simon Fraser University, Burnaby, BC, Canada, [4]UK Atomic Energy Authority, Abingdon, UK

SFU SIMON FRASER UNIVERSITY · TRIUMF · UK Atomic Energy Authority

25th Topical Conference on High Temperature Plasma Diagnostics, Asheville, NC, April 21-25, 2024, **Poster 3.4.45**

INTRODUCTION: THE LM26 PROGRAM

General Fusion (GF) is developing its next-generation Magnetized Target Fusion (MTF) experiments under the LM26 (Lawson Machine 2026) project.

The aim of LM26 is to validate the company's ability to symmetrically compress magnetized plasmas in a repeatable manner and achieve fusion conditions at scale. It will demonstrate plasma heating by compressing a solid lithium liner driven by a magnetic θ-pinch. A magnetized plasma target will be compressed to a temperature of 10 keV by 2025. It is then designed to progress towards scientific breakeven equivalent conditions by 2026.

To confirm the scientific results of this program, the LM26 machine will require a wide range of diagnostics systems to measure the key plasma parameters, such as electron density (n_e), electron (T_e) and ion (T_i) temperature and energy confinement time (τ_E). See posters 4.2.1, 4.2.22 for details.

Due to the presence of a moving metal liner (expected to reach its full radial compression ratio of 10:1 within a few ms of the initial pulse), available room for diagnostic sensors is limited to a progressively smaller surface area during a compression shot, up until peak compression where only the center shaft and its immediate surroundings will face the plasma. These conditions and requirements therefore require a careful strategy to ensure that LM26 plasmas can be diagnosed adequately at all stages of compression.

Fig. 1: Prototype schematic of the LM26 design, highlighting the Marshall gun used for Coaxial Helicity Injection (CHI) to the left, and the high-vacuum target chamber surrounded by a solid lithium liner to the right. Diagnostic systems are expected to be installed on the conical sections of the center shaft, as well as in the disposable central section.

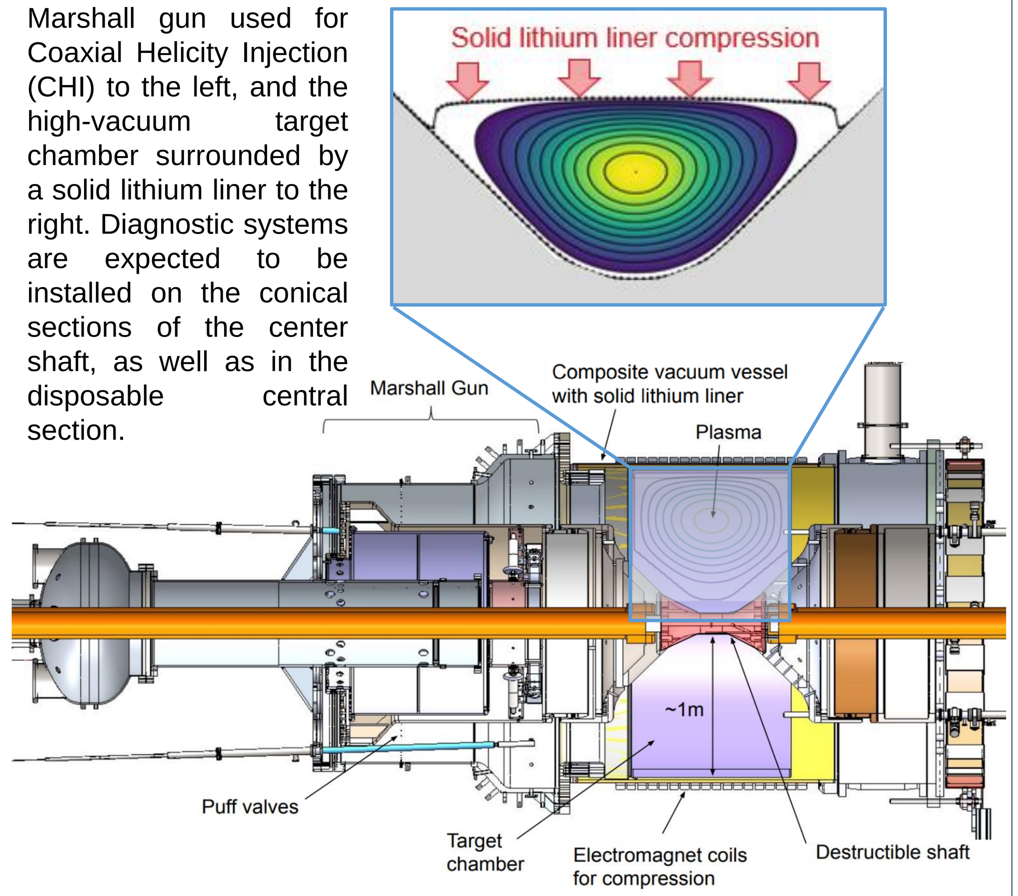

LM26 NEUTRON EMISSION

LM26 will compress a deuterium plasma and produce the following fusion reaction with a 50% branching ratio:

$$D + D \rightarrow {}^3_2He + n(2.45\ MeV)$$

Simulations of the LM26 liner and plasma compression produce equilibrium values from which the neutron rate is determined as a function of compression time. Figure 2 shows the simulated plasma temperature profiles for two times in compression when the peak plasma reaches 1 keV (Fig. 2(a)) and 10 keV (Fig. 2(b)). The LM26 center shaft is drawn in black along the bottom and the collapsing lithium liner is drawn in blue. Figure 3 shows the evolution of the peak ion temperature and the neutron emission rate during compression. The total neutron yield from LM26 during a compression shot is predicted to be 6.6x10^{12} neutrons. The peak neutron rate when the ion temperature reaches 10 keV is predicted to be 4.0x10^{17} neutrons/s. These values are specific to the machine geometry and the plasma and liner compression trajectory that were simulated and may change as these simulations develop.

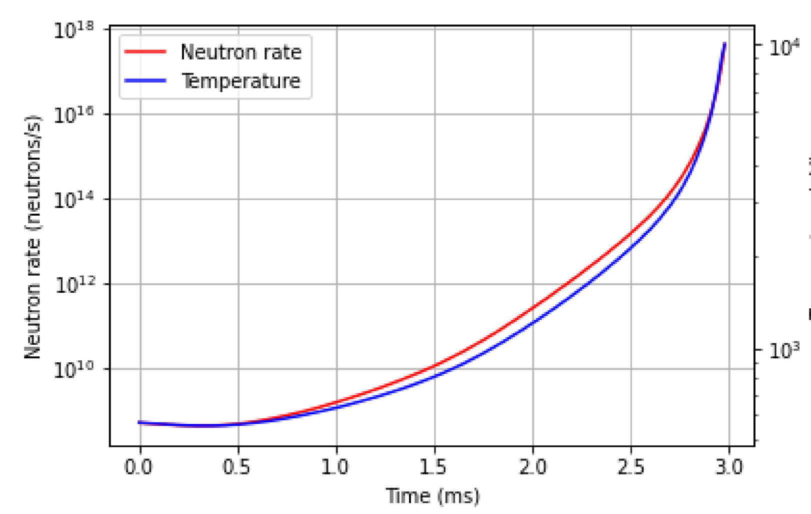

Fig. 3: Neutron emission rate and peak ion temperature as a function of the time of compression of LM26.

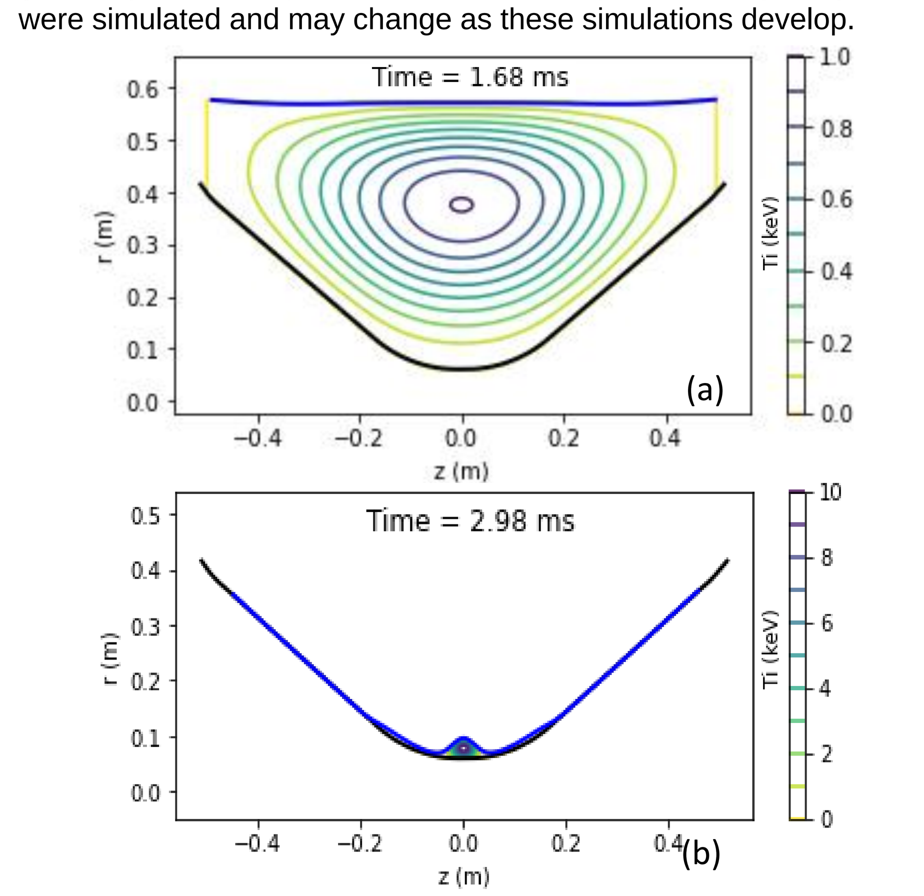

Fig. 2: Plasma temperature profiles during compression; (a) time 1.68 ms when peak plasma temperature is 1 keV; (b) time 2.98 ms when peak plasma is 10 keV

T$_i$ MEASUREMENT

Fusion neutrons emerging from an MTF plasma will have a Gaussian energy distribution that is a function of the temperature of the reacting ions,

$$\sigma_{T_i} = \frac{82.5\sqrt{T_i}}{2\sqrt{2\ln(2)}}$$

where σ_{T_i} is the neutron energy distribution standard deviation in keV and T_i is in keV. This behavior is shown in Figure 4.

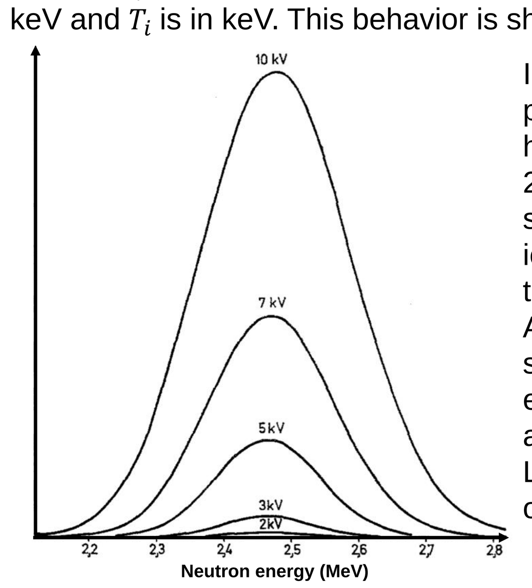

In the case of a deuterium plasma, the fusion neutrons have an average energy of 2.45 MeV with a thermal spread due to the plasma ion temperature from which the fusion reaction occurred. An advantage of this MTF scheme is that the neutron energy spectrum should be a simple Gaussian since LM26 has no neutral beam or radio-frequency heating.

Fig. 4: Neutron energy distributions for increasing plasma temperatures. Adapted from [1].

NEUTRON SPECTROMETER

A neutron spectrometer measures the spread in the neutron energy distribution to estimate T_i. General Fusion, in partnership with TRIUMF, Simon Fraser University and Université de Sherbrooke has received funding through a four-year NSERC Alliance grant, to develop and build a neutron spectrometer to measure 10 keV plasma temperature at LM26 with a resolution of 20% or better. A mock design is shown in Figure 5 [2]. Ion temperature measurements are a critical parameter to evaluate compression performance.

A direct line-of-sight to the compressed plasma as it is heated to 10 keV is achieved via a chord through the LM26 center shaft, extending out of the machine to the spectrometer (Figures 6, 7).

Fig. 5. Simplified model of a multi-layer time-of-flight spectrometer. The incident and scattered neutron trajectories through the scintillator layers are shown in red [2].

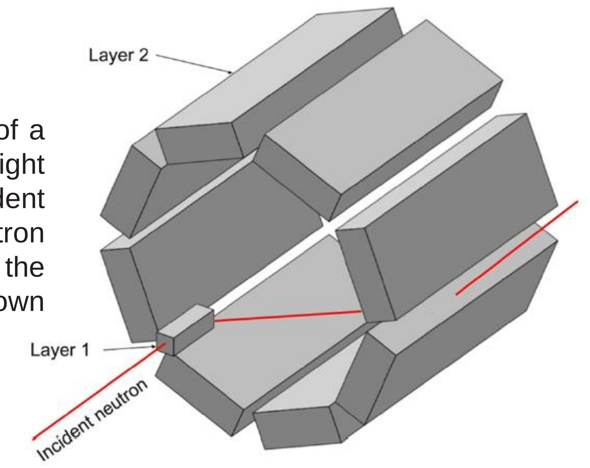

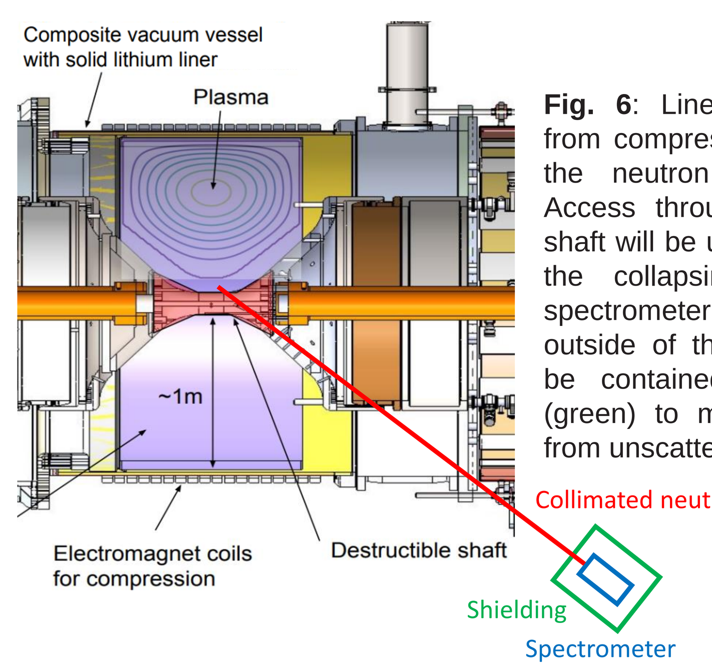

Fig. 6: Line-of-sight chord from compressed plasma to the neutron spectrometer. Access through the center shaft will be unobstructed by the collapsing liner. The spectrometer (blue) located outside of the machine will be contained in shielding (green) to maximize signal from unscattered neutrons.

Fig. 7: Zoomed-in view of the intersection of the spectrometer chord (red) with the compressed plasma at 10 keV.

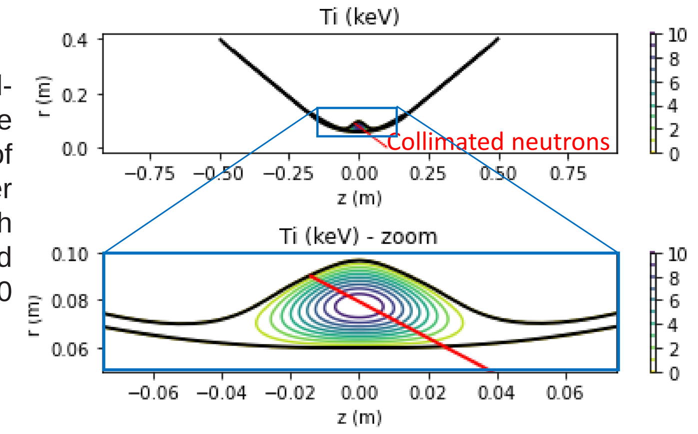

TIME-OF-FLIGHT (TOF)

A neutron emitted from the plasma with initial energy E_n will elastically scatter in the first detector layer, with a resulting energy E_n' proportional to its scattering angle, θ:

$$E_n' = E_n \cos^2\theta$$

The scattered neutron can interact with the second detector layer. The time between interactions (t_{TOF}) and path length between interaction points ($R^2 + Z^2$), the initial neutron energy can be calculated:

$$E_n = \frac{m_n(R^2 + Z^2)^2}{2Z^2 t_{TOF}^2}$$

To achieve a Ti measurement with a resolution σ_{T_i} better than 20%, the Z-position resolution must be 1 cm or better, t_{TOF} resolution must be 150 ps (353 ps FWHM).

CONCEPTUAL DESIGN

Time-of-flight (TOF) neutron spectrometry has been used as a neutron diagnostic system to measure fusion reaction rates and plasma temperature at facilities including JET [3, 4] and NIF [5]. The design of the spectrometer follows that of TOFOR at JET with two layers of detectors to determine the energy of the incident neutron (Figure 5). The conceptual design of the neutron spectrometer is shown in Figure 8 [2].

To handle the high incident neutron flux at the spectrometer, layer 1 will be segmented into ~60 plastic scintillator segments, individually wrapped and coupled to a silicon photomultiplier (SiPM) for light readout. Layer 2 will be composed of 8 modules of ~64 long plastic scintillator bars. The time difference in the light readout at opposite ends of the bars will determine the neutron interaction point on the bar, which is required to calculate the flight path length.

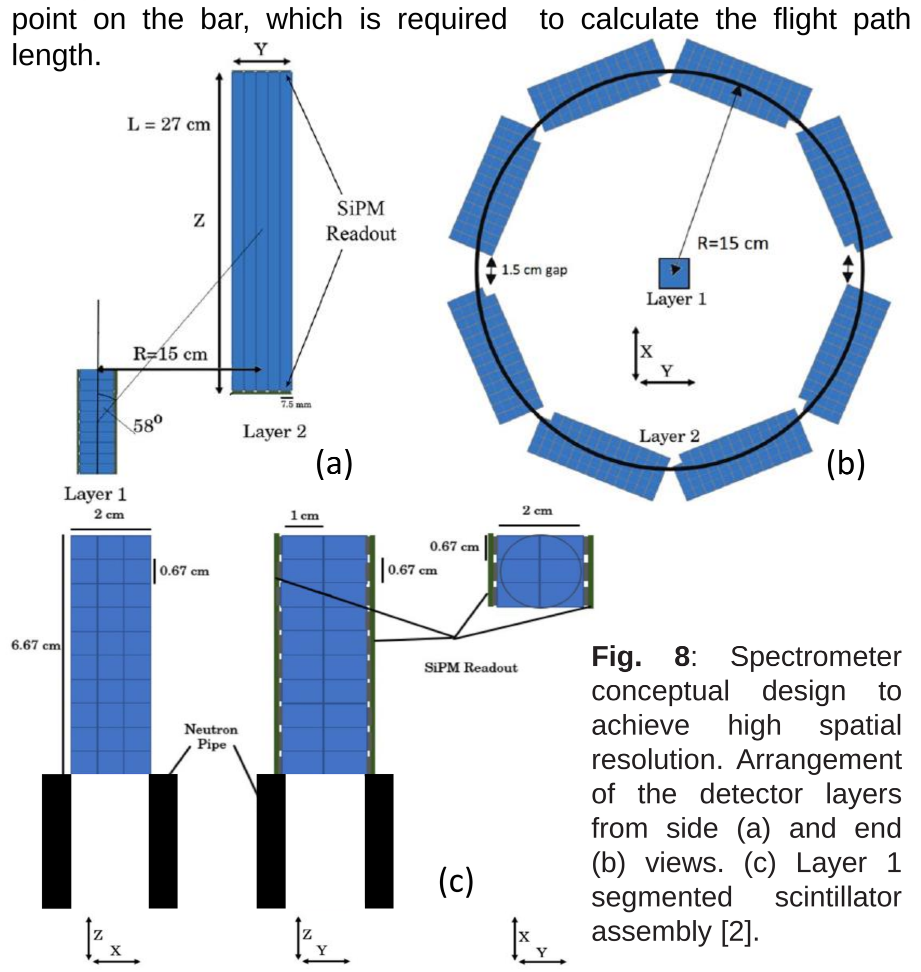

Fig. 8: Spectrometer conceptual design to achieve high spatial resolution. Arrangement of the detector layers from side (a) and end (b) views. (c) Layer 1 segmented scintillator assembly [2].

COMPONENT TESTING

Small-scale component tests are being performed at TRIUMF, Canada's particle accelerator centre. Components of interest are listed in Table 1. Deliverables from these tests include:

- Single photon timing resolution (SPTR) of SiPM + readout electronics
- Timing resolution of the layer 1 and 2 scintillators
- Position resolution along layer 2 scintillator bar
- Gamma-ray energy deposition in scintillator (Figure 9)
- Neutron energy deposition in scintillator

Fig. 9: Test setup with ^{22}Na gamma ray source. Collimated 511-keV gammas will scatter in plastic scintillator. Barium fluoride (BaF_2) will be a time-timing reference. Deposited energy will be measured with cerium bromide ($CeBr_3$).

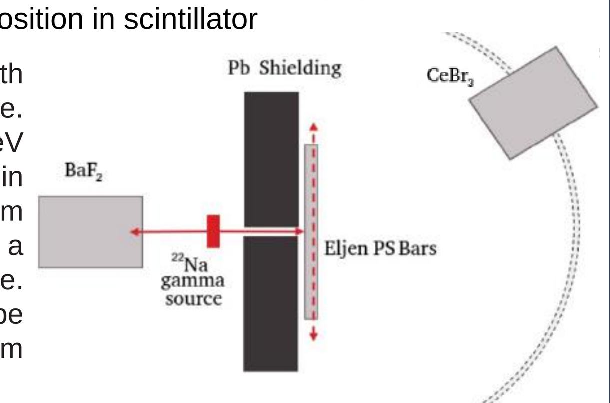

Table 1: Spectrometer components under investigation.

Plastic Scintillator		
Layer 1	EJ-232Q	Ultra-fast: < 110 ps rise time, 700 ps decay time
Layer 2	EJ-230	Good light yield, light attenuation length
Silicon Photomultiplier (SiPM) Light Collection		
Broadcom NUV-MT	4 mm, 6 mm	~55% PDE at 370 nm, reduced dark count rate
Readout Electronics: CAEN		
A5203 with picoTDC	~7 ps timing resolution, Time-over-Threshold (ToT) based analysis, scalable to >1000 channels	
A5204 with picoTDC + Radioroc 2 ASIC		

NEUTRON COUNTING DIAGNOSTICS

Additional neutron diagnostic systems are being considered for use on LM26. The diagnostic suite will have detection capabilities to span the expected range of neutron emission rates, from start-up to 10 keV operation.

Liquid Scintillators

- Neutron-gamma pulse shape discrimination (PSD) (Figure 10)
- Time-resolved response
- Currently in use on General Fusion's Plasma Injector 3 (PI3)
- Predicted to become saturated at 10 keV operating point

Helium-3 Proportional Counters

- Gamma-insensitive
- Time-independent verification of neutron yield
- Future collaboration with Canadian Nuclear Laboratories (CNL)

Indium Foil Activation

- $^{115}In(n, n')$ reaction produces ^{115m}In daughter nucleus with half-life of 4.5 hours
- High energy resolution, shielded HPGe detector measures 336 keV gamma ray rate from ^{115m}In decay
- Gamma-insensitive
- Time-independent verification of neutron yield

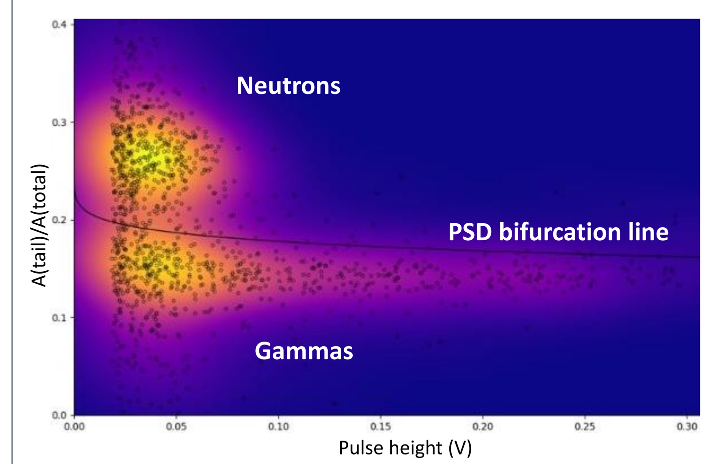

Fig. 10: Pulse shape discrimination (PSD) from a liquid scintillator (EJ-301) at PI3.

UKAEA NEUTRONICS VALIDATION

A neutronics validation program with the UK Atomic Energy Authority is underway [6]. A simplified model of LM26 and surrounding components in the experimental hall was created (Figure 11). MCNP neutron transport simulations were performed with a neutron source term originating from General Fusion's plasma compression simulations (Figure 12). The resulting neutron and photon fluence maps of the experimental hall are shown in Figures 13 and 14.

The responses of the following diagnostic systems will be calculated for the 10 keV peak compression scenario, as well as lower peak plasma temperatures, to map the expected diagnostic response during operational phases:

- Neutron spectrometer
- Liquid scintillators
- Helium-3 counters
- Indium activation foils
- Fission counters

Fig. 11: Simplified model of LM26 and capacitor banks in the experimental hall.

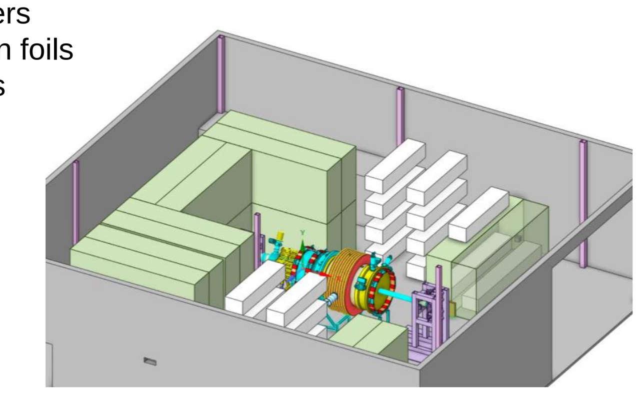

Fig. 12: Source particle locations within LM26 for MCNP simulations.

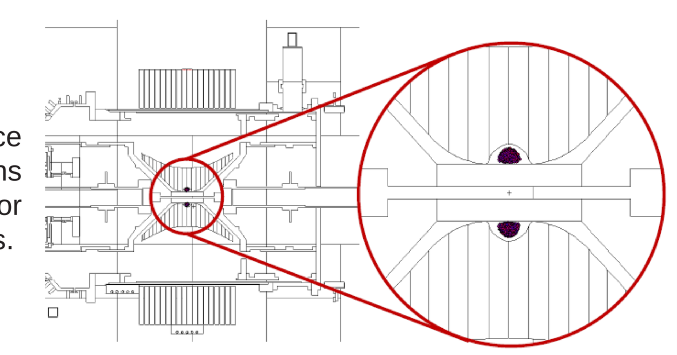

UKAEA NEUTRONICS VALIDATION

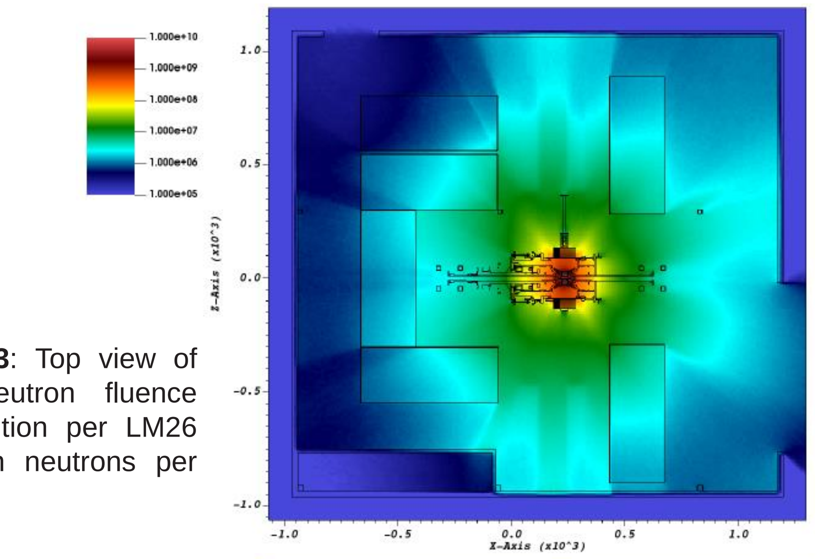

Fig. 13: Top view of the neutron fluence distribution per LM26 shot in neutrons per cm^2.

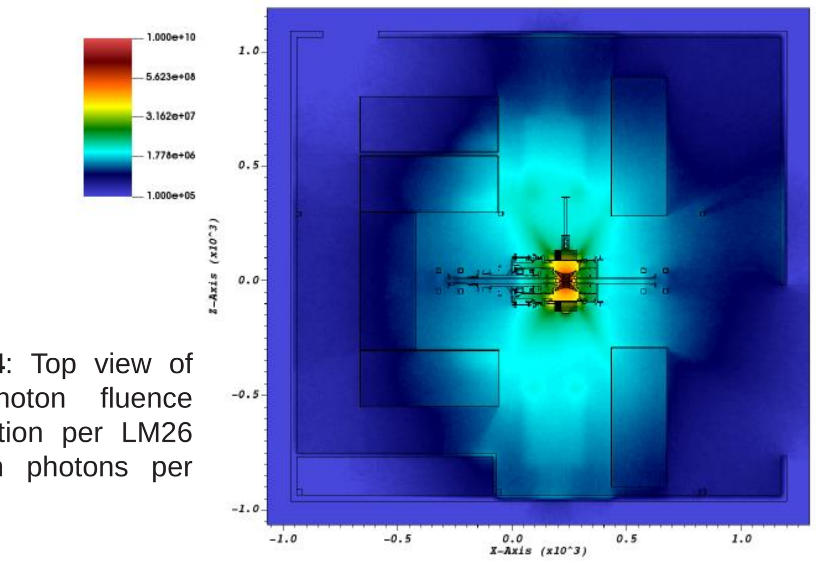

Fig. 14: Top view of the photon fluence distribution per LM26 shot in photons per cm^2.

CONCLUSIONS & FUTURE WORK

The neutron spectrometer, as well as additional neutron counting diagnostics, will be used to evaluate the performance of a plasma compression shot at LM26 and calculate the plasma temperature with an uncertainty better than 20%.

A multi-institution collaboration with General Fusion is developing a neutron spectrometer to perform high-resolution plasma temperature measurements. LM26 will compress plasmas to 10 keV and the neutron spectrometer will have line-of-sight access to the 2.45 MeV neutrons from deuterium-deuterium fusion. A two-layer, highly segmented spectrometer composed of plastic scintillators will use time-of-flight to measure the energy distribution of neutrons emitted from the 10 keV plasma. The distribution is a function of the plasma temperature.

Future work includes:

Continuation of UKAEA neutronics simulations:

- Optimize diagnostic placement and operational dynamic range
- Calculate incident and scattered neutron and gamma ray rates at the neutron spectrometer
- Optimize neutron spectrometer shielding configuration

Neutron Spectrometer:

- GEANT4 neutron spectrometer simulations:
  - Layer 1 and layer 2 scintillator response to expected incident neutron flux
  - Incorporation of experimental results of timing and position resolution, energy deposition
- Mult--segment scintillator assembly:
  - Scintillator wrapping and assembly methods
  - Optical crosstalk measurements

REFERENCES

[1] G. Lehner, F. Pohl, Z. Physik, 207(1), 83-104 (1967)
[2] P. Carle et al. Rev. Sci. Instrum. 93, 113539 (2022)
[3] A. Hjalmarsson et al. Rev. Sci. Instrum. 74, 1750 (2003)
[4] M. Gatu Johnson et al. Rev. Sci. Instrum. 77 10E702 (2006)
[5] A. S. Moore et al. Rev. Sci. Instrum. 92, 023516 (2021)
[6] UKAEA neutronics simulations internal report to General Fusion (2024)

We acknowledge the support of the Natural Sciences and Engineering Research Council of Canada (NSERC).